Available online at www.sciencedirect.com

ScienceDirect

Procedia Structural Integrity 59 (2024) 11–16

Structural Integrity Procedia

www.elsevier.com/locate/procedia

VII International Conference "In-service Damage of Materials: Diagnostics and Prediction" (DMDP 2023)

Bending Tests of Pre-Stressed Concrete Rail Sleepers

Gabriella Bolzon[a]*, Andrea Collina[b], Mohammad Hajjar[a], Emanuele Zappa[b]

[a]*Department of Civil & Environmental Engineering, Politecnico di Milano, Piazza Leonardo da Vinci 32, 20133 Milano, Italy*
[b]*Department of Mechanical Engineering, Politecnico di Milano, Via Giuseppe La Masa 1, 20156 Milano, Italy*

Abstract

Sleepers are railway elements subjected to demanding working conditions and strict structural requirements. The acceptance procedures proposed by standard EN 13230-2 for concrete sleepers include the execution of a sequence of static 3-Point Bending Tests. In each step, the maximum applied force is increased by a pre-fixed amount. As a main crack is detected, the corresponding width and residual opening displacement are measured. This kind of testing was performed in previous research work, monitoring fracture propagation by Digital Image Correlation (DIC). This contribution considers a different experimental setup and procedure, consisting of a 4-Point Bending Test with a continuous loading-unloading process. The deformation of the central portion of the sleeper, subjected to uniform bending, and the fracture pattern are monitored by DIC also in this case. The results demonstrate the substantial equivalence of the two alternative approaches compared here for the evaluation of the in-service mechanical performance of these structural elements.

Keywords: Sleepers; Pre-stressed Concrete; Bending test; Digital Image Correlation; In-service performance

1. Introduction

Sleepers are railway elements subjected to demanding working conditions and strict structural requirements related to safety. Railway sleepers are pre-stressed concrete elements, with an expected service life of more than 50

* Corresponding author. Tel.: +39-02.2399.4319
E-mail address: gabriella.bolzon@polimi.it

10.1016/j.prostr.2024.04.003

years. Their main loading condition is typically represented by a couple of vertical loads transferred by the train wheel through the rail interactions, balanced by the reaction coming from the contact pressure exchanged with the underneath ballast. The unevenness of the ballast degradation in the long term, can subsequently modify the distribution of the bending along the sleeper. The resulting bending moments on the sleeper can initiate cracks, which propagate with the transit of trains. Fracture processes may also be promoted by local damages produced by accidental impact loads, e.g. due to the intervention of tamping machines, to the transit of defected wheels with a wheel-flat, or to the breakage of poorly maintained joints.

The mechanical resistance of railway sleepers to these external actions is commonly evaluated by 3-Point Bending Test (3PBT) performed on full-scale samples, according to standard EN 13230-2 (2016). The suggested stepwise loading procedure assumes that the applied forces are progressively increased by a pre-fixed amount. At each step, the opening of the main crack is measured. Aim of the static tests is to assess the design value required for the centerline section and for the section in correspondence of the rail seat.

3PBT produces maximum bending under the applied load, where the initial fracture position is expected to be localized. Nevertheless, complex fracture patterns are observed on pre-stressed sleepers, as for instance shown by Carboni et al. (2018, 2020), Liu et al. (2020), Silva et al. (2020). The crack position can be determined uniquely by introducing notches, as done for example by Rezaie and Farnam (2015). However, this provision alters the overall strength of the tested elements, and the bending moment for crack initiation.

The alternative 4-Point Bending Test (4PBT) is frequently used to assess the structural performance of concrete members failing by fracture propagation (ASTM C78/C78M-18, 2018). 4PBT produces a region of uniform bending, where cracks develop in pure opening mode, with no shear contribution. Additionally, 4PBT avoids localized compressive damage, which can develop under the load application points. Focusing on the centerline section test, it is worth recalling that the bending moment in this area is not related to the application of a force on the centerline section, but to the rotation of the lateral portions of the sleepers under the rail seat, associated to an uneven settlement of the ballast. The bending is enforced by vertical forces associated to the transit of the wheelset, and uneven distribution of the reaction pressure under the rail seat areas. As a conclusion, the 4PBT appears to be closer to the real operating condition.

In all cases, the formation and propagation of fracture can be monitored by optical means during the loading process. In pre-stressed elements, cracks can close almost completely upon unloading. Therefore, the fracture position and extent can hardly be detected after the test, unless the sample is led to complete failure.

In this contribution, the results of static 3PBT performed according to the standards are compared with the outcome of continuous loading-unloading processes in 4PBT configuration. All tested elements are monitored by high resolution cameras, and 3D Digital Image Correlation (DIC) is adopted as the process to detect the presence of cracks also at the early stages and to measure their aperture, where they are hardly visible.

2. Experimental work

The experimental setup considered in the present work is schematized in Fig. 1.

Static load is applied by a 300 kN servo-hydraulic actuator, controlled in force. The load in increased either in stepwise ramps (in 3PB, according to standards), or continuously (in 4PB), at a rate of 120 kN/min. Articulated supports and rubber pads are placed under the sleeper in correspondence of the supports, and at the load application points, in order to prevent local damages in the concrete elements due to local indentation of the supports against the concrete sleeper surface

A vision-based measurement system monitors the deformation of the sample and the crack propagation during the test. Two GX3300 digital cameras equipped with a 4/3” CCD sensor (8MPixel) and Zeiss lenses of 50 mm optical length are mounted on tripods placed in the front of the sleeper, to face the area where cracks are most likely to appear. The regions of interest (much larger in the case of 4PBT) are also visualized in Fig. 1 as shaded areas.

The cameras are controlled by means of a custom-made software developed in National Instruments LabVIEW environment, synchronized through a shared trigger signal provided with a waveform generator. A stereo camera calibration procedure is carried out in order to compensate for perspective distortion, and to recover all the intrinsic and extrinsic parameters, to finally obtain the 3D maps of displacement and strain in engineering units.

The tests performed according to the international standard EN 13230-2 (2016) are described in detail by Carboni et al. (2018, 2020). An initial value of the applied force is defined by the standards, depending on the sleeper class. The load is then incremented sequentially by a fixed amount (in this case, 10 kN), and kept constant during time intervals 10 s to 5 min long, while the presence of crack(s) is detected and the width of the main one is measured. The standards define the main crack as the first one that propagates at a distance of more than 15mm from the bottom edge of the sleeper.

The presence of cracks is evidenced by large (though immaterial) localized values of the strain field, which is evaluated by finite differences starting from the displacement distribution acquired by DIC. The crack opening is obtained as the difference between the horizontal displacement components of two points across a discontinuity position at a relative distance that depends on the width of the monitored region and on the number of available measurement data, in order to overcome the experimental noises.

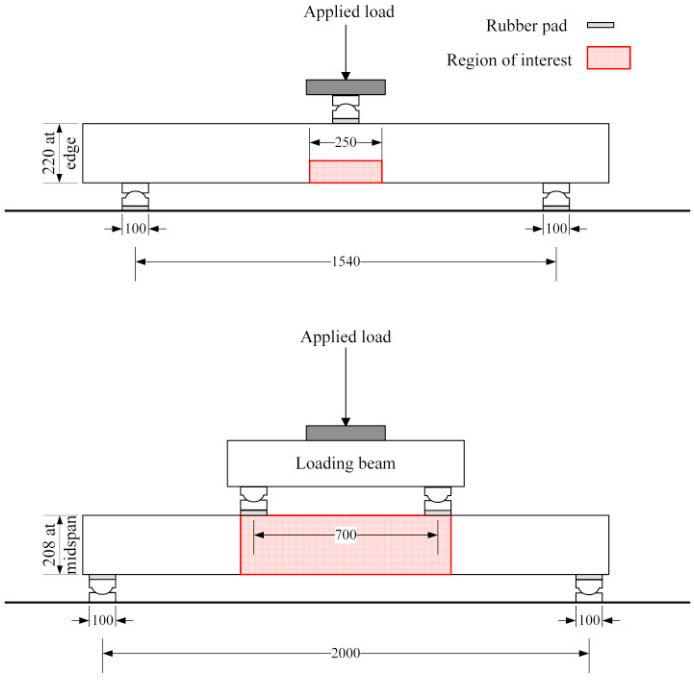

Fig. 1: Schematic of the experimental setup for the considered 3PBT and 4PBT.

In 4PBT, a steel beam is used to evenly distribute the force over the two loading plates shown in Fig. 1. Three triangulation laser sensors (OPTO NCDT 1302-50) measure the vertical displacements at the two supports and at the mid-span section. In this way, the net deflection of the specimen can be calculated, compensating the deformations of the rubber pads at the supports. The results are then compared to the DIC output. Images are taken at 1 Hz frequency and processed all together at the end of the test. Load-displacement data, fracture patterns and crack profiles are acquired continuously.

3. Experimental results

The main results collected from 3PBT and 4PBT of pre-stressed sleepers designed for the same railway application are summarized in this section. The different configurations are compared in terms of maximum bending moment, in one case produced at mid-span, in the other as uniform value between the loading plates of the tested samples.

Multiple branching cracks are observed in all cases. Branching is commonly induced by the biaxial stress-state that develop at the crack tip as fracture propagates in bent elements (Bolzon and Cocchetti, 1998).

3-Point Bending Test (3PBT)

Carboni et al. (2018) performed 3PBT of pre-stressed sleepers, following the stepwise loading process and crack identification procedure suggested by the standard EN 13230-2 (2016). The main results are summarized in Table 1.

Table 1. Main results of 3PBT performed by Carboni et al. (2018).

Load [kN]	Bending Moment [kNm]	Event
63	24	First visible crack
73	28	Multiple cracks
97	37	Crack branching
122	47	Complete failure

The first visible crack is observed at about 63kN force, while complete failure occurs at about 122 kN. These loads correspond to the maximum bending moment of about 24 kNm and 47 kNm for the considered experimental setup, see Fig. 1.

The width of cracks detected by visual inspection is estimated as 0.04 mm (Liu et al., 2020). Notably, the standards associate this measure to the elastic limit.

The snapshot in Fig. 2 shows the fracture scenario at about 98 kN applied load. The branching of the main crack and the presence of a secondary crack are clearly visible.

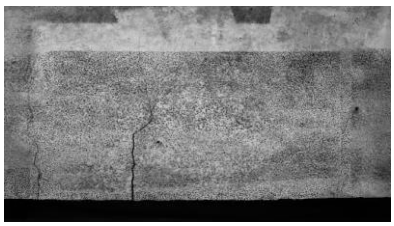

Fig. 2: Snapshot of the region of interest of the 3PBT sketched in Fig. 1 at about 98kN applied load.

4-Point Bending Test (4PBT)

The force applied to samples subjected to 4PBT is increased continuously by 120 kN/min rate up to 120 kN, and then removed. The load-deflection and bending-deflection curves of two samples are shown in Fig. 3. Free unloading is allowed in one case (sample S1), load-controlled in another case (S2), where a cycle of partial unloading and reloading is also performed.

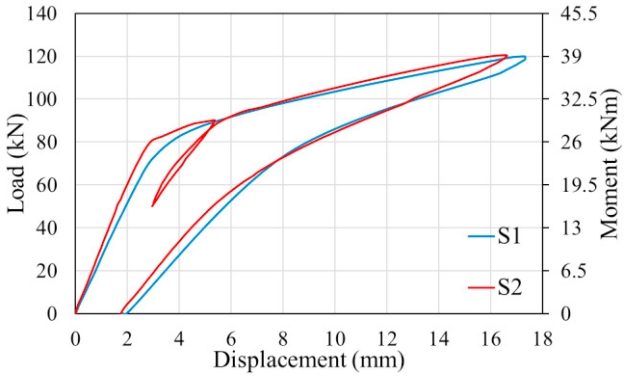

Fig. 3: Load-deflection curve in 4PBT of samples S1 and S2.

Multiple cracks in a different number appear since the beginning of the test, and propagate more or less to the same extent as the external load is increased. Their relative position is shown in Fig. 4, which visualizes the map of the horizontal strains recovered by DIC at the maximum load. The strain map at unloading is also shown in Fig. 4 (notice the different color scale).

At the maximum load (120 kN) the sleeper height is almost completely crossed by the cracks although the samples do not reach complete failure. On the other hand, the corresponding bending moment (39 kNm) is lower than the maximum value achieved in 3PBT (45 kNm).

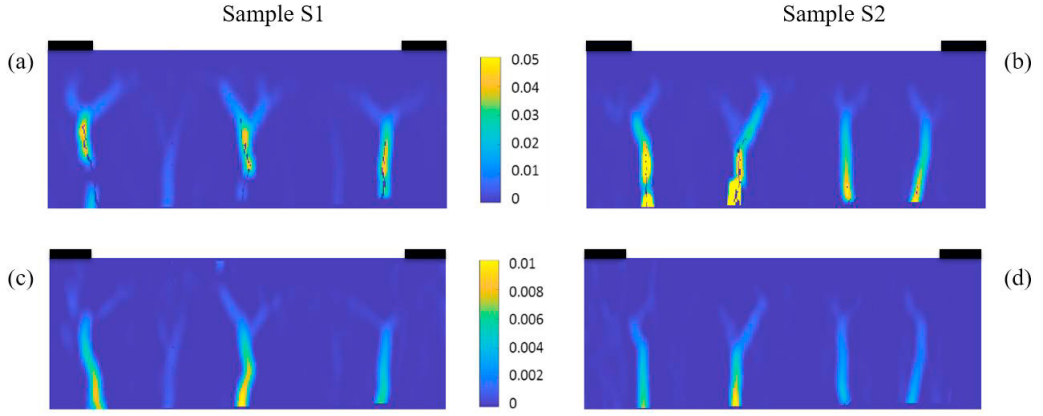

Fig. 4: Maps of the horizontal strains produced by 4PBTs at the maximum load (a, b) and at unloading (c, d); not in real scale.

Fig. 5 displays the profile of the fractures developing in sample S2 in the range 50 kN to 90 kN of the applied force. The main loading path (L1), partial reloading (L2), and complete unloading are represented. The opening displacements are extracted from the recorded set of images collected during the whole experiment, and processed by DIC at the end of the test.

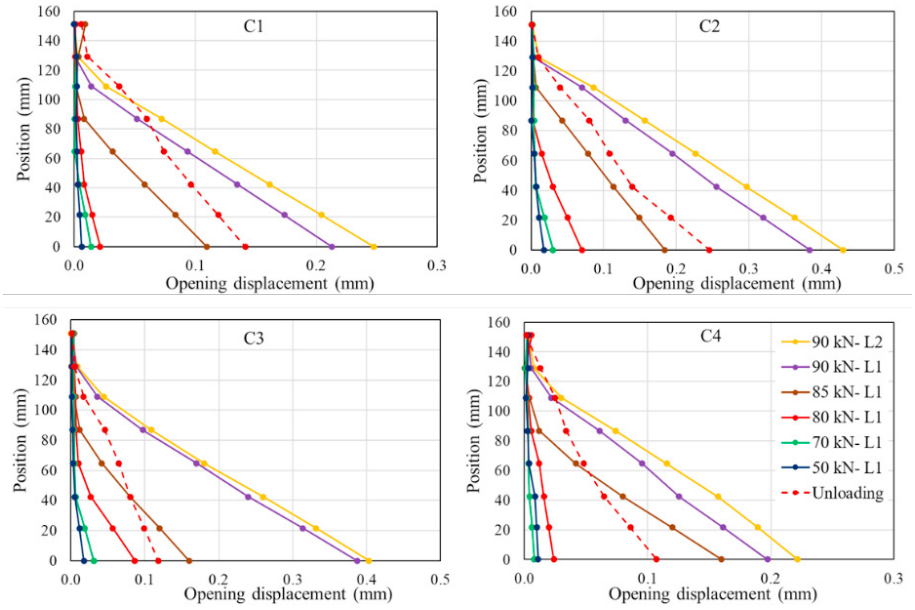

Fig. 5: Opening profiles of the cracks developing in sample S2; different horizontal scale for the central (C2, C3) and lateral (C1, C4) cracks. Position (in ordinate) indicates the distance from the bottom edge of the sleeper.

Crack C3 reaches about 0.04 mm opening displacement (visible threshold) at about 75 kN applied force (i.e., 24 kNm bending moment), consistently with the 3PBT results reported by Carboni et al. (2018), summarized in Table 1. Roughly, this bending level corresponds to the end of the initial linear branch of the load-displacement curves represented in Fig. 3. However, the graphs in Fig. 5 evidence that the actual elastic threshold is below 50 kN force.

The crack opening rate increases above 80 kN applied force (26 kNm bending moment), likely identifying the loss of the initial cohesion in concrete. This structural change is reflected also by the significant reduction of the slope of the (almost bilinear) loading curve of Fig. 3.

Crack branching occurs at about 90 kN (29 kNm bending). It is worth noticing that multiple cracks are also reported in 3PBT in the interval 26-29 kNm.

Finally, it can be observed that the relative displacements on the fracture surfaces increase after unloading and reloading, while the residual crack opening at complete unloading is of the order of 0.1-0.2 mm.

4. Conclusion

This contribution aims at comparing the results of 3-Point Bending Tests (3PBTs) and 4-Point Bending Tests (4PBTs) carried out on pre-stressed concrete sleepers. The sample deformation and fracture processes are monitored by digital image correlation (DIC) technique in all cases. The results demonstrate the substantial equivalence of the two alternative approaches considered here in identifying the most significant events occurring during the experiments, and the corresponding load levels. However, the performed 4PBT procedure is faster, since a single load ramp is performed. The collected information, which includes the whole load-unloading curves, provides interesting information on the evolution of the material status, and on the different load carrying mechanisms developing in the sleeper during the test.

Acknowledgements

The Authors would like to thank Nicola Sautto for his assistance during the execution of the tests.

References

ASTM C78/C78M-18, 2018. Standard Test Method for Flexural Strength of Concrete (Using Simple Beam with Third-Point Loading). ASTM International, West Conshohocken, PA, USA.

Bolzon, G., Cocchetti, G., 1998. On a case of crack path bifurcation in cohesive materials. Archive of Applied Mechanics 68, 513–523.

Carboni, M., Collina, A., Liu, R., Zappa, E., 2018. A preliminary feasibility analysis about the structural health monitoring of railway concrete sleepers by acoustic emission and digital image correlation. International Symposium on Structural Health Monitoring and Nondestructive Testing, Saarbruecken, Germany.

Carboni, M., Collina, A., Zappa, E., 2020. An acoustic emission-based approach to structural health monitoring of pre-stressed concrete railway sleepers. Insight 62(5), 1–12.

EN 13230-2, 2016. Railway applications – Track – Concrete sleepers and bearers – Part 2: Pre-stressed monoblock sleepers. European Standardization Organization, Bruxelles.

De Wilder, K., Lava, P., Debruyne, D., Wang, Y., De Roeck, G., Vandewalle, L., 2015. Experimental investigation on the shear capacity of prestressed concrete beams using digital image correlation. Engineering Structures 82, 82–92.

Hajjar, M., Bolzon, G., Zappa, E., 2023. Experimental and numerical analysis of fracture in prestressed concrete. Procedia Structural Integrity 47, 354–358.

Liu, R., Zappa, E., Collina, A., 2020. Vision-based measurement of crack generation and evolution during static testing of concrete sleepers. Engineering Fracture Mechanics 224, 106715.

Silva, R., Silva, W., Farias J., Santos, M., Neiva, L., 2020. Experimental and numerical analyses of the failure of prestressed concrete railway sleepers. Materials 13, 1704.